Multi-Resolution Image Morphing

Manfred Kopp and Werner Purgathofer

Vienna University of Technology, Institute of Computer Graphics,
Karlsplatz 13/186-2, A-1040 Wien, Austria
{kopp | wp}@cg.tuwien.ac.at
http://www.cg.tuwien.ac.at/research/ca/mrm/

Abstract

The proposed technique extends conventional image morphing algorithms by offering additional control over the processing of the individual multi-resolutions that are used in the wavelet representation when moving from the source to the destination image. This gives the animator the possibility to introduce a disparity between the morphing of global and detail features that can lead to interesting new effects that are not achievable with traditional methods.

The calculation of an intermediate image in conventional image morphing algorithms is done in three steps: firstly the determination of feature correspondence and of an intermediate feature geometry, secondly the warping of the source and the destination images to intermediate images that match the feature geometry, and finally the blending of the two warped images. The proposed algorithm alters the third step by making the blending dependent on the multi-resolution levels using a new specialized 2D wavelet transformation.

Keywords: Animation, Image Morphing, Wavelets

1. Introduction

Image morphing, sometimes also called image metamorphosis, deals with the smooth transformation from one digital image to another. This technique is often used in the entertainment industry to achieve stunning special effects. Image morphing is a combination of image warping with a cross-dissolve between image elements. The main idea of this technique is the following: Given a source and a destination image with corresponding features, calculate an intermediate image by warping the source and the destination to images where the corresponding features are aligned, and then cross-dissolving between these two warped images. As the animation proceeds, the source image is smoothly faded out and distorted towards the alignment of features in the destination image. The destination image starts distorted to the feature geometry of the source image and while it fades in, the distortion is gradually reduced. Therefore the first images of the sequence are much like the source image, while the last images are similar to the destination image. The middle image of the animation contains an average of the source and the destination image adjusted to an average feature geometry.

1.1 Related Work

Different approaches have been reported in literature for the specification of the corresponding features and generating the distorted warpings for the calculation of the intermediate images: In mesh based warpings, such as the technique proposed by Wolberg [1] and Nishita et al. [2], the feature geometry in the source and destination picture are specified by the distortion of a regular grid. An extension of this technique is proposed by Lee et al. [3] who use a multi-resolution approach with a hierarchy of control lattices for the definition of the deformation functions. The conventional mesh based techniques provide fast and intuitive warpings, which can be easily supported by image processing hardware. However, these conventional mesh based methods have a common drawback in specifying the features in an image as reported in [4]. An alternative approach for the specification of the warping deformation called field morphing was introduced by Beier and Neely [4]. In this approach corresponding geometric entities like 2D lines or curves are specified in the source and in the destination image and interpolated for the intermediate images. The warped images are calculated by a weighted average of pixels in the local coordinate system of the specification lines or curves, where the weights are indirectly proportional to the distance from the specification entity. This technique provides an easy to use interface for the specification of the corresponding features at the cost of greater computational cost, which is proportional to the number of geometric entities times the number of pixels in the image. The

multi-resolution grid methods proposed in [3][5] also use geometric entities for the specification of the corresponding features and utilize the grids only for efficient internal computation.
Even with an intuitive user interface, the time for the interactive design of the morphing sequence is much higher than the actual computation of the morphing itself. In [4], Beier and Neely reported that the interactive design time for a morphing sequence is about 10 times higher than the computation of the final frames. Due to the fast increase of computational power, this relationship is getting even worse. Therefore, image processing techniques for detecting the corresponding features are used to speed up the design cycle. A very promising approach in this direction is proposed by Lee et al. [3], who use an image processing technique called “snakes” for semi-automatic feature recognition.
An other extension to the conventional morphing algorithm called view morphing, introduced by Seitz and Dyer [6], deals with the case of differing 3D projective camera settings of the source and the destination images. In conventional morphing algorithms, only 2D transitions between images are used, which result in unnatural morphings if the 3D camera parameters are not the same in the source and the destination image. To overcome this visual defect, the morphing algorithm is extended with a pre- and a post-processing pass for adjustment to the different camera parameters: In the preprocessing part, a pre-warping of the source and the destination image is performed to generate intermediate images with parallel camera views. The pre-warping transformation is computed using corresponding 3D points, which have to be specified in both images. The pre-warped images are morphed with conventional 2D techniques and then post-warped to interpolated camera settings.
Similar morphing techniques were proposed for the smooth transition of 3D voxel based objects. A problem with direct interpolation of the warped source and destination volume in the spatial domain is that the high frequency components of the source and the destination volume often cause unsatisfactory results in the morphing sequence. Therefore, the morphing is performed in the Fourier [7] or wavelet domains [8] to reduce high frequency distortion: The high frequency components of the source volume are quickly faded out while the high frequency components of the destination volume are faded in slowly. Therefore the sum of the two blending factors for high frequency components in the intermediate volumes is less than 100%, which sometimes generates some blocking artifacts.

1.2 Motivation and Overview

In this paper, an extension to the image morphing algorithms is proposed, which utilizes the multi-resolution levels of the wavelet transformation to gain control over the blending of the warped images in the different frequency bands. Figure 1 illustrates the effects on the morphing animation gained by this additional degree of freedom: If the wavelet coefficients of the finer levels, which correspond to the detail information in the image, have a faster transition from the source image, the Mona Lisa painting, to the destination image, the computer generated thorny-head picture, than the wavelet coefficients of the coarser levels, peaked thorns pop out very quickly in the animation and the landscape is blurred gradually. In the opposite multiresolution parameter setting, if the wavelet coefficients of coarser levels, corresponding to the global features, have a higher transition rate, the landscape fades to white quickly, but sharp contours are still visible until a short time before the destination image is reached. Also the

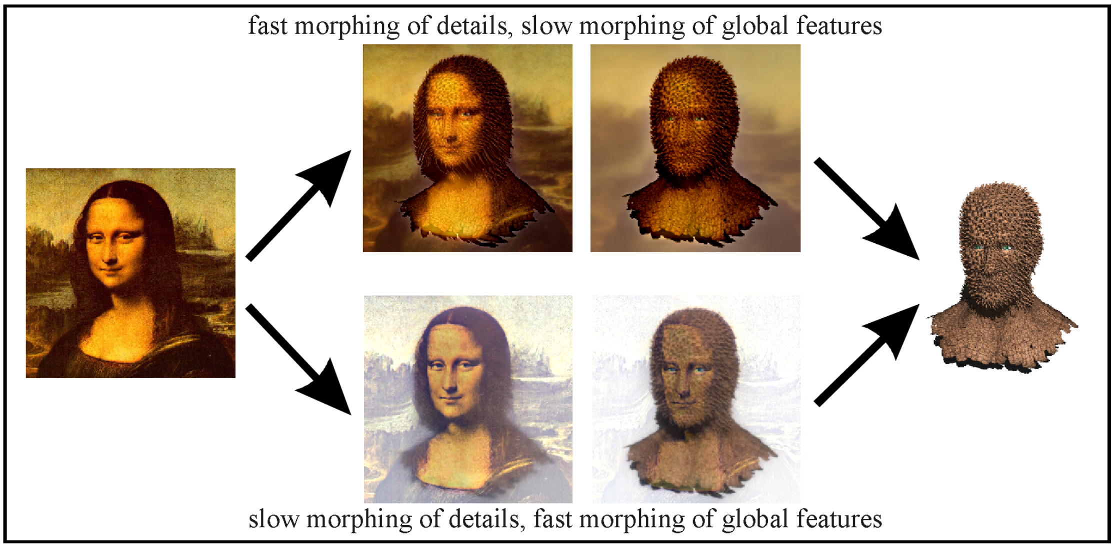

Figure 1: Morphing with different multiresolution parameters

animated face generates a completely different impression: The thorns emerge slowly from boils. These interesting effects can not be achieved with conventional morphing algorithms. The goal of this paper is to present an extension to the image morphing algorithms, where the animator has easy the additional posibility to specify the transition of details versus global features in some specified regions.

Section 2 gives a brief overview of wavelet theory and introduces a new decomposition scheme for 2D wavelets, where the computational cost per multi-resolution level is lower than in conventional decomposition schemes. Section 3 deals with the multi-resolution extension of conventional morphing algorithms. A general image morphing framework is introduced and user interface issues for the definition of the multi-resolution blending functions are discussed. Section 4 describes the details of the actual implementation of the proposed method. In section 5, results of the proposed morphing extension are presented and section 6 summarizes the proposed extension of the morphing algorithm.

2. Wavelets for Image Morphing

In the recent years, wavelet based methods have gained importance in many different fields of computer graphics including wavelet radiosity [9], multi-resolution painting [10], curve design [11], mesh optimization [12], volume visualization [13], image searching [14], variational modeling [15], and object compression [16]. Overviews of wavelet based algorithms for computer graphics can be found in [17][18]. This section contains only a brief introduction to the theory of wavelets seen from the filtering point of view, more details of the mathematical definitions can be found in [19][20].

2.1 Wavelet Transformation in 1D

Let s_n denote a signal with 2^n regularly spaced sample points. In one transformation step of the fast wavelet transformation, an analysis filter pair with a low pass filter $\overline{h}_k$ and a high pass filter $\overline{g}_k$ is applied to the signal and downsampling by a factor 2 is performed. This results in a coarser resolution of the signal s_{n-1} with 2^{n-1} sample points, which are called smoothing or scaling coefficients, and 2^{n-1} detail or wavelet coefficients d_{n-1}, which contain the missing details of the signal s_n which can not be represented in the coarser resolution s_{n-1}. This transformation step is applied recursively on the scaling coefficients. This results in a multi-resolution representation of the signal with one scaling coefficient over the whole range, and all 2^i detail coefficients d_i with the multi-resolution level i ranging from 0 to (n-1). It has been proven in wavelet theory, that if these filter pairs correspond to a biorthogonal multi-resolution analysis, e.g. quadrature mirror filters [20], there exists a dual filter pair h_k and g_k with which an exact reconstruction can be achieved using the inverse wavelet transformation:

$$s_{i,k} = \sum_m h_{k-2m} s_{i-1,m} + g_{k-2m} d_{i-1,m} \tag{1}$$

Figure 2 illustrates one transformation step of the wavelet transformation (2a) and the inverse wavelet transformation (2b).

If the filter pairs are compactly supported, which means that the filters have only finite extent, the wavelet transformation and the inverse wavelet transformation can be done in linear time proportional to the number of sample points times the filter length.

One frequently encountered problem which has not been mentioned yet, occurs when the signal is not periodic and only defined within a certain interval, but the filters used need values outside of this specified region. Simple solutions to this problem are zero padding, making the signal periodic, or, if the corresponding wavelet function of the multi-resolution analysis is symmetric or anti-symmetric, mirroring at the borders. A more sophisticated approach to this problem is to use different filters for the calculation of the coefficients at the borders [20].

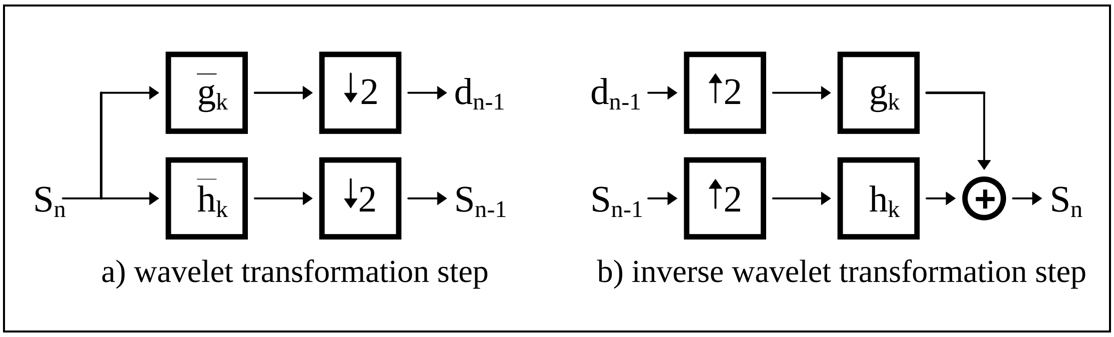

Figure 2: diagram of the wavelet and inverse wavelet transformation steps

2.2 Wavelet Transformation in 2D

Since we want to use the wavelet transformation on images, we need to extend the method to 2D. There are different approaches to be found in the literature which extend wavelets to higher dimensions. The dilatation matrix methods use 2D filters and sublattices in Z^2 instead of the simple subsampling to extend the wavelets to 2D [21]. The quincunx scheme with the dilatation matrix $D = \begin{pmatrix} 1 & 1 \\ 1 & -1 \end{pmatrix}$, or stated otherwise, with $DZ^2=\{(m,n);\, m+n \in 2Z\}$, is one of the most promising methods in the class of dilatation matrix based wavelets.

The second approach are separable methods that extend the wavelet transformation to higher dimensions by applying the 1D filters to each dimension. There are two methods reported in literature, which use this type of extension to higher dimensions [20]: The *standard* or *rectangular decomposition* consists of two passes: First a 1D wavelet transformation is independently performed on every row of the image. In the second pass, a 1D wavelet transformation on every column is applied to the row wavelet transformed image. Figure 3a demonstrates this technique with a simple 16x16 image. The left and upper parts contain the smoothing coefficients, the right and lower parts the wavelet coefficients of the row- and column wavelet transformation, respectively. Note that the wavelet coefficients may also contain negative values, and therefore 0 is mapped to 50% gray.

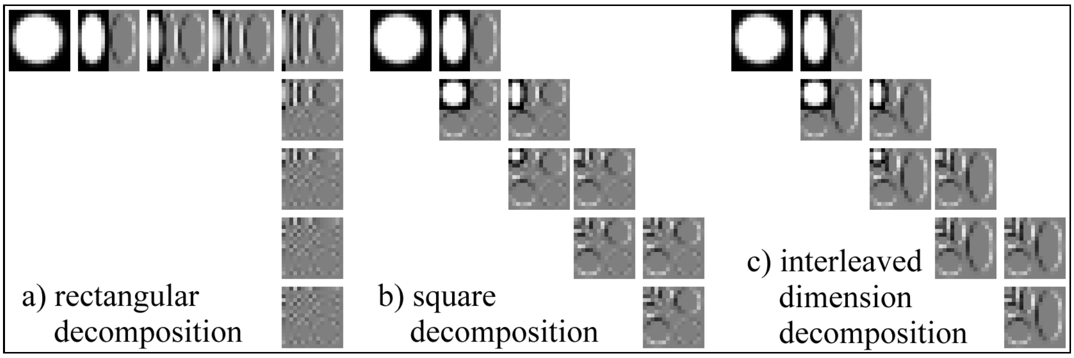

Figure 3: 2D wavelet decomposition schemes

The *nonstandard* or *square decomposition* applies the row and column wavelet transformation steps in an interleaved way. Figure 3b illustrates this technique: First a row transformation step is applied to every row. Then a column transformation step is performed on the intermediate coefficients. These two steps are performed recursively on the remaining smoothing coefficients in the upper left corner. Note that less operations are needed for the square decomposition than for the rectangular decomposition and that the spatial influence of the wavelet coefficients is a square, if the 1D filter pair has the same extent.

2.3 Interleaved Dimension Decomposition

One disadvantage of the square decomposition is the fact, that between one level of the wavelet coefficients to the next coarser level, there is a dilatation factor of 2 in every dimension, resulting in a spatial influence 4 times bigger than in the finer level. In our application, a high number of multiresolution levels, which is indirect proportional to the area dilatation factor, is desired: The multiresolution extension is based on a different weighting of the coefficients in different multiresolution level. The animator specifies the transition in some key multiresolution levels, for

example the finest and coarsest level, and the other transitions are interpolated. To avoid artifacts, the change of the weighting of successive levels should be small. Therefore, better quality can be achieved with more intermediate multiresolution levels.
To overcome the disadvantage of few multi-resolution levels of the nonstandard decomposition, a new 2D decomposition method is proposed, the *interleaved dimension decomposition*: The interleaved dimension decomposition is very similar to the square decomposition, but generates intermediate multi-resolution levels: First a row transformation step is performed as in the square decomposition, but in contrast to the square decomposition, the following column transformation is only performed on the smoothing coefficients of the row transformation step. As in the square decomposition, these two transformation steps are applied recursively to the remaining smoothing coefficients. Figure 3c illustrates the difference to the square decomposition in 3b with a simple 16x16 image. There is a close relationship between the square decomposition and the interleaved dimension decomposition: The intermediate scaling coefficients and 1/3 of the wavelet coefficients are the same as in the square decomposition. The other 2/3 of the wavelet coefficients, which represent the intermediate multi-resolution levels, are wavelet coefficients of a square decomposition of a transformed version of the original image that is scaled by a factor of two along the *y*-Axis. The order of applying the 1D wavelet transformation steps in the different dimensions can be chosen arbitrarily; this leads to two different decompositions in 2D: row first, as described in this paragraph and shown in figure 3c, or column first. Note also, that the computation time of the interleaved dimension decomposition is lower than that of the square decomposition.

2.4 Desired Properties for the 2D Wavelets for Image Morphing

The multi-resolution image morphing approach uses the wavelet coefficients for the image blending operation instead of the pixel values in conventional morphing algorithms. Since the animator wants to manipulate the morphing based on different multi-resolution levels, there should be as many multi-resolution levels as possible. The square decomposition with an area dilatation factor of 4 from one level to the next is therefore not the best choice. The rectangular decomposition provides more different multi-resolution levels, but at the cost of very unbalanced spatial influence of the coefficients. The quincunx scheme has an area dilatation factor of 2 from one level to the next, but the disadvantage of this scheme is the high computational cost, which is $O(p \cdot m^2)$, where m is the filter length in one dimension and p is the number of pixels, while separable methods only need $O(p \cdot m)$ operations. The interleaved dimension decomposition is well suited to the application of multi-resolution morphing, since it is the fastest 2D wavelet decomposition method and provides an area dilatation factor of 2.
For the choice of the wavelet filters, the following properties are desired:

- **Short compact support of the analysis and reconstruction filters**: The filter length is directly proportional to the computation time of the wavelet transformation and the inverse wavelet transformation.
- **Smoothness:** If the corresponding scaling functions and wavelet functions are not smooth, disturbing artifacts will reduce the resulting image quality. If biorthogonal wavelets are used, the smoothness of the synthesis wavelets and scaling functions are important for the image quality.
- **Filters with dyadic rational coefficients:** Fixed point arithmetic can be used if the filters have only dyadic rational coefficients. Fixed point arithmetic can save memory space and on most computers, it is also faster than floating point arithmetic.

Unfortunately, the first two points are not independent of each other, which means that wavelet and scaling functions with higher smoothness are only possible with longer corresponding filters. Therefore, a tradeoff between computation time versus image quality has to be made.

3. Multiresolution Image Morphing

3.1 General Image Morphing Framework

This framework extends the approach by Lee et al. in [5] by using the multi-resolution extension to morphing proposed in this paper.
Let I_0 and I_1 be the source and the destination image, respectively. Let F_0 and F_1 be two sets of corresponding features specified by the animator on I_0 and I_1, respectively. We define the warp functions W_0 and W_1 as distortion functions that map any point in I_0 and I_1 to the corresponding point in I_1 and I_0, respectively. When W_0 is applied to the image I_0, denoted as $W_0 \bullet I_0$, it generates a distorted

image of I_0 with the features $f_0 \in F_0$ aligned to the features $f_1 \in F_1$. Similarly, $W_1 \bullet I_1$ generates a distorted image of I_1 with the features $f_1 \in F_1$ aligned to the features $f_0 \in F_0$.
In contrast to the image morphing framework in [5], we propose to use two different types of transition functions, which also have different input parameters:

The geometry transition functions: $T_0^{geom}(p,t)$ and $T_1^{geom}(p,t)$, which are dependent on the coefficient position p and the time t, are used to generate the smooth warping sequences from I_0 and I_1 to their distorted feature aligned counterparts $W_0 \bullet I_0$ and $W_1 \bullet I_1$, respectively. In [5], these geometry transition functions are also used for the blending operation. They also explain how the dependency on the position p can be used for local control of the geometric distortion.

The blending transition functions: $T_0^{blend}(p,i,t)$ and $T_1^{blend}(p,i,t)$ control the color composition based on the wavelet coefficients and are dependent on the position p and multi-resolution level i of the wavelet coefficients and also on the time t. If $T_0^{blend}(p,i,t)$ and $T_1^{blend}(p,i,t)$ are only dependent on p and t and not on i, the conventional approach with blending of the pixel values can be used and no wavelet transformations need to be performed.

Let $WT \circ I$ denote the 2D wavelet transformation applied to the image I and $WT^{-1} \circ \bar{I}$ the inverse 2D wavelet transformation applied to the image $\bar{I}$ in wavelet domain, then the morphing procedure can be written formally with the following formulas:

$$\overline{W_0}\ (p,t) = \left(1 - T_0^{geom}(p,t)\right) \cdot p + T_0^{geom}(p,t) \cdot W_0(p) \tag{2}$$

$$\overline{W_1}\ (p,t) = T_1^{geom}(p,t) \cdot p + \left(1 - T_1^{geom}(p,t)\right) \cdot W_1(p) \tag{3}$$

$$\bar{I}_0(p,i,t) = \overline{W_0}\ (p,t) \bullet \left(\left(1 - T_0^{blend}(p,i,t)\right) \cdot WT \circ I_0(p)\right) \tag{4}$$

$$\bar{I}_1(p,i,t) = \overline{W_1}\ (p,t) \bullet \left(T_1^{blend}(p,i,t) \cdot WT \circ I_1(p)\right) \tag{5}$$

$$I(p,t) = WT^{-1} \circ \left(\bar{I}_0(p,i,t) + \bar{I}_1(p,i,t)\right) \tag{6}$$

Equation (2) and (3) define the warping functions, (4) and (5) apply the blending to the wavelet transformed images and distort the image in wavelet space according to the warping functions and (6) performs the composition and inverse wavelet transformation. Note that the warping is done in wavelet space and is dependent on the relative position of the coefficients, but not on the multi-resolution level. A dependency between the warping and the multi-resolution levels would generate misaligned multi-resolutions that lead to distracting artifacts.
The general image morphing framework can be extended to include also the view morphing approach by applying a prewarping on the source and destination images I_0 an I_1 and a postwarping on the result in (6) according to the camera parameter as described in [6].

3.2 Multi-Resolution based Blending Transitions

The multi-resolution behavior of the morphing in the presented general image morphing framework can be controlled by the blending transition function. Since the influence of the two images I_0 and I_1 should sum up to 100%, there is an inherent constraint between T_0^{blend} and T_1^{blend}: For each wavelet coefficient in I_1 with position p_1 and multi-resolution level i, $T_1^{blend}(p_1,i,t)$ is defined to have the same transition rate as $T_0^{blend}(p_0,i,t)$ if p_0 corresponds to p_1 in I_0. Therefore T_1^{blend} is completely determined by T_0^{blend} and only one of these two functions has to be specified.
The main user interface issue for the specification of the blending transition is not to restrict the power of the whole function too much, but let the animator achieve his goals in very few steps.
We will first consider a simpler case, where the blending is not dependent on the position. Let the time t be normalized to lie in [0,1] and the transition functions also generate values in [0,1]. For any multi-resolution level i, $T_0^{blend}(i,0)$ and $T_0^{blend}(i,1)$ are equal to 0 and 1, respectively. For values of t between 0 and 1, $T_0^{blend}(i,t)$ should be a smooth function for every multi-resolution level i. Also the difference between the transitions from one multi-resolution level to the next should not be too high to avoid

artifacts. Since in most cases the animator wants to specify only some specific transitions of selected multi-resolution levels, the intermediate transition functions should be calculated by interpolation. An example for this kind of functions are bias functions: only one bias value is needed for the definition of the transition function for one level and interpolated transition functions can be easily computed by interpolation of the bias values. Since the bias function has an undesired high slope for high bias values, we used a modified function:

$$transition(b,t) = \begin{cases} bias(b,t) & \ldots 0 \le b < 0.5 \\ 1 - bias(1-b, 1-t) & \ldots 0.5 \le b \le 1 \end{cases} \quad (7)$$

Like the bias function, this transition also has the property:

$$transition(b, \tfrac{1}{2}) = b \quad \ldots\ 0 \le b \le 1 \quad (8)$$

A good user interface for the blending transition that also takes the coefficient position into account is more difficult to design. To gain access to the whole power of our approach a blending curve has to be specified for every coefficient. Even if the curves are specified only by a few reference coefficients, this would burden the animator with a tediously large number of manual adjustments.

We propose the following method for the multiresolution blending transition: The animator generates a gray scale image of the transition of details in the source image, which we call detail transition map. The pixels in the detail transition map define the parameter b in the transition function (7) for each wavelet coefficient of the highest level in the corresponding position. For the coarsest multiresolution level a negated detail transition map is computed and for the other multiresolution levels the map is interpolated. Since the resolution of the wavelets of the coarser levels is lower than the resolution of the finer levels, the corresponding maps also need only the coarser resolution.

4. Implementation

The multi-resolution extension to image morphing was implemented on a PC using the Linux operating system and X-Windows. We used the morphing algorithm by Beier and Neely [4] as the basis for the multi-resolution extension, which provides an easy to handle user interface for the definition of the features. The program applies the interleaved dimension decomposition described in chapter 2.3 for the 2D decomposition of the wavelets. Different types of 1D wavelets for the 2D decomposition were examined. The Haar wavelets, which are the simplest type of wavelets, are very fast to compute, but yielded very bad results. In contrast, the family of biorthogonal symmetric spline wavelets, described in [20], generated excellent morphing animations even with the simplest type of this family of wavelets, the ${}_{1,3}\psi$ wavelet with a support width of the filters of 2 and 6, respectively. Also cubic Battle-Lemarié wavelets and Pseudocoiflets were examined.

5. Results

Figure 4 shows four morphing sequences with images of the authors, one photograph and one computer generated pastel. The first row shows the morphing sequence with pixel-blending based morphing. The second and third row use global multiresolution transition functions, while the last row is generated by locally dependent transition functions. The second row shows the resulting animation for fast transition of the finer multiresolution levels, corresponding to the details, and slow transition of the coarser levels, corresponding to the global features. The third row has the reverse settings with fast transition of the coarser levels and slow transition of the finer levels. The detail transition map of the morphing sequence in the fourth row is black (,corresponds slow transition of details in this region) on the left side, white (, corresponds fast transition) on the right side and has small horizontal linear ramp in the middle. Figure 5 shows morphing sequences with a typical computer generated ray tracing image and a photograph and figure 6 displays morphing sequences with two photographs. Figure 7 shows the results of different wavelets of the middle image in the morphing animation of figure 5 with slow detail transition. Only the Haar wavelet produce visible artifacts, all others produce hardly distinguishable results. Therefore the fastest, the symmetric biorthogonal ${}_{1,3}\psi$ wavelet with a support width of the filters of 2 and 6 were choosen for the generation of morphing sequences in figure 4-6.

6. Conclusions

An extension to the 2D image morphing algorithm was introduced that gives the animator control over the behavior of the image morphing in terms of detail versus global characteristics. This enhancement improves the flexibility of the specification of the morphing behavior in a way that is not achievable with conventional techniques. A new 2D wavelet decomposition method called interleaved dimension decomposition was also introduced, which is better suited to the application of multi-resolution image morphing than conventional approaches. A general image morphing framework was presented, which includes 3D camera transformations, spatial dependent transition behavior and the proposed multi-resolution control. Some user interface issues about the definition of the multi-resolution blending transitions was discussed. The implementation, which produced visually attractive results, was carried out on standard PC hardware.

7. Acknowledgments

The Authors want to thank Andreas Artmann and Gerhard Waldhör for help with the implementation of the X-Multiresolution Morphing, Robert Tobler and Wolfgang Meyer for the photographs and Kurt Fleischer, David Laidlaw, Bena Currin and Alan Barr at California Institute of Technology for the Thorny-Head image.

8. References

[1] Wolberg, George. Digital Image Warping. IEEE Computer Society Press, Los Alamitos, CA, 1990

[2] Nishita, Tomoyuki, Toshihisa Fujii, and Eihachiro Nakamae. Metamorphosis Using Bezier Clipping. In Proceedings of the First Pacific Conference on Computer Graphics and Applications (Seoul, Korea, 1993), World Scientific Publishing Co., pp. 162–173.

[3] Lee, Seung-Yong, Kyung-Yong Chwa , Sung Yong Shin, and George Wolberg. Image metamorphosis using snakes and free-form deformations. Proc. SIGGRAPH´95. In Computer Graphics (1995), pp. 439–448.

[4] Beier,T.,and Neely, S. Feature-based image metamorphosis. Proc. SIGGRAPH´92. In Computer Graphics (1992), pp. 35–42.

[5] Lee, Seung-Yong, Kyung-Yong Chwa, James Hahn, and Sung Yong Shin. Image Morphing Using Deformation Techniques. The Journal of Visualization and Computer Animation 7, 1 (1996), pp. 3-23

[6] Seitz, Steven M., Dyer, Charles R. View Morphing. Proc. SIGGRAPH 96. In Computer Graphics (1996), pp. 21–30.

[7] Hughes, John F. Scheduled Fourier Volume Morphing. Proc. SIGGRAPH 92. In Computer Graphics (1992), pp. 43-46.

[8] He, Taosong, Wang, Sidney, Kaufmann, Arie. Wavelet-Based Volume Morphing. Proceedings Visualization ´94, Washington DC, IEEE Computer Society Press, October 1994, pp. 85-92.

[9] Steven Gortler, Peter Schröder, Michael Cohen, Pat Hanrahan, "Wavelet Radiosity", Computer Graphics, Annual Conference Series (Siggraph'93 Proceedings), pp. 221-230, 1993

[10] Deborah Berman, Jason Bartell, David Salesin, "Multiresolution Painting and Compositing", Computer Graphics, Annual Conference Series (Siggraph'94 Proceedings), pp. 85-90, 1994

[11] Adam Finkelstein, David Salesin, "Multiresolution Curves", Computer Graphics, Annual Conference Series (Siggraph'94 Proceedings), pp. 261-268, 1994

[12] Matthias Eck, Tony DeRose, Tom Duchamp, Hugues Hoppe, Michael Lounsberry, Werner Stuetzle, "Multiresolution Analysis of Arbitrary Meshes", Computer Graphics, Annual Conference Series (Siggraph'95 Proceedings), pp. 173-182, 1995

[13] L. Lippert, M. Gross, "Fast Wavelet Based Volume Rendering by Accumulation of Transparent Texture Maps", Eurographics'95 Conference Proceedings, Computer Graphics Forum Vol. 14, Nr. 3, pp. 431-443, 1995

[14] Charles Jacobs, Adam Finkelstein, David Salesin, "Fast Multiresolution Image Querying", Computer Graphics, Annual Conference Series (Siggraph'95 Proceedings), pp. 277-286, 1995

[15] Zicheng Liu, Steven Gortler, Michael Cohen, "Hierarchical Spacetime Control", Computer Graphics, Annual Conference Series (Siggraph'94 Proceedings), pp. 35-42, 1994

[16] Andrew Certain, Jovan Popovic, Tony DeRose, Tom Duchamp, David Salesin, Werner Stuetzle, Interactive Multiresolution Surface Viewing, Computer Graphics, Annual Conference Series (Siggraph'96 Proceedings), pp. 91-98, 1996

[17] Eric J. Stollnitz, Tony D. DeRose, David H. Salesin, Wavelets for Computer Graphics - Theory and Applications, Morgan Kaufmann Publishers Inc., San Francisco, California, 1996
[18] Peter Schröder, Wim Sweldens, Michael Cohen, Tony DeRose, David Salesin, Wavelets in Computer Graphics, SIGGRAPH 96 Course Notes
[19] Charles K. Chui, "An Introduction to Wavelets", Academic Press Inc., Boston, MA 1992
[20] Ingrid Daubechies, "Ten Lectures on Wavelets", Vol. 61 of CBMS-NSF Regional Conference Series in Applied Mathematics, SIAM, Philadelphia, PA 1992
[21] J. Kovacevic, M. Vetterli, Nonseperable multidimensional perfect reconstruction filter banks and wavelet bases for R^n, IEEE Transactions on Information Theory, Vol. 38, pp. 533-555, 1992

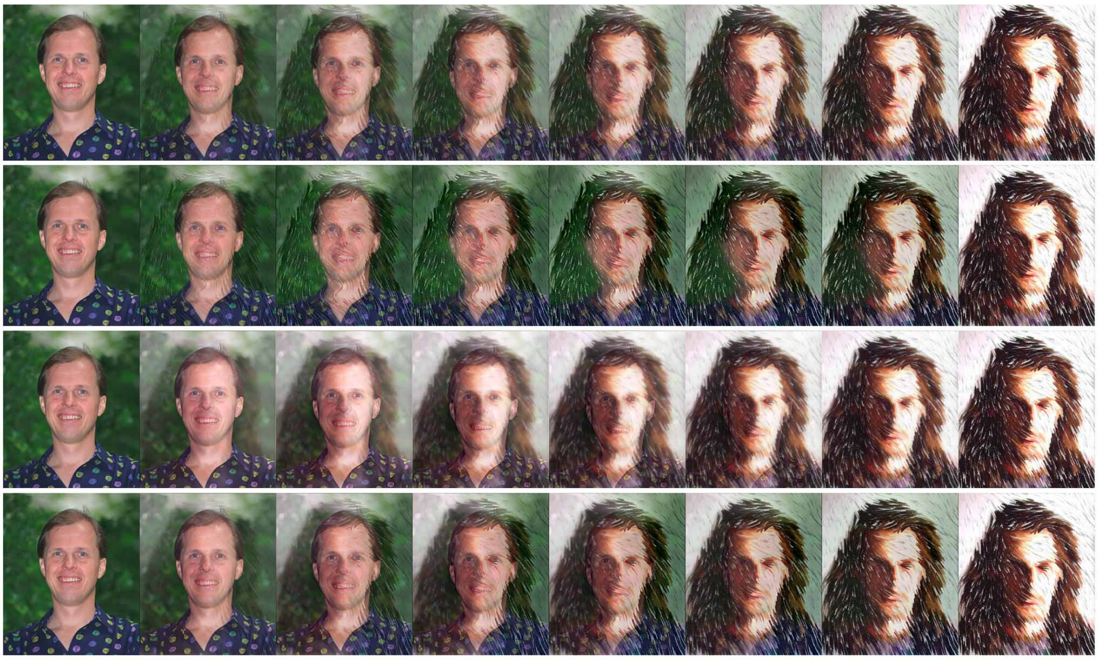

Figure 4: image morphing with different multiresolution transition functions: first row - conventional morphing; second row - fast morphing of details; third row - slow morphing of details; fourth row - spatial dependent multiresolution transition

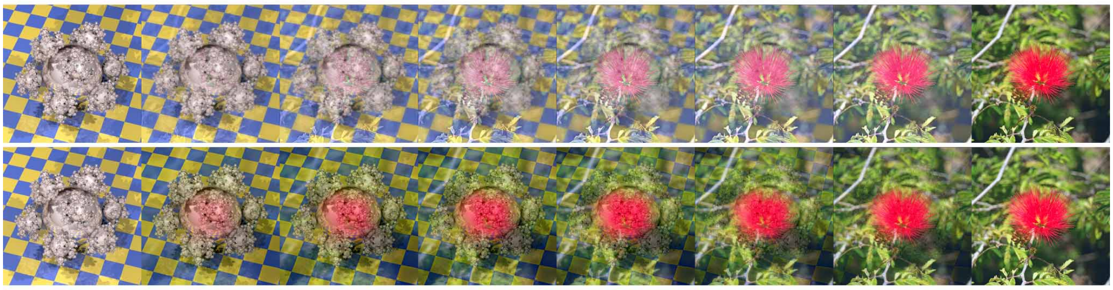

Figure 5: first row: morphing with fast transition of details and slow transition of global features; second row: morphing with slow transition of details and fast transition of global features

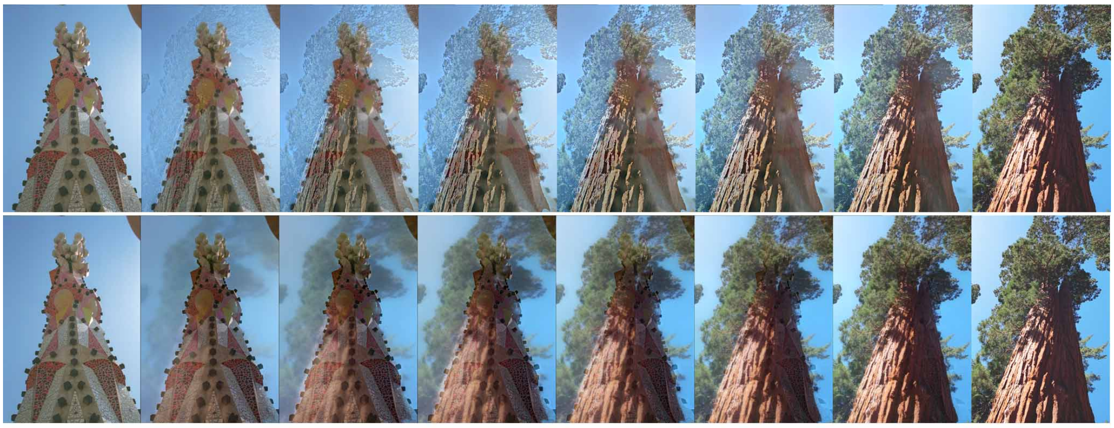

Figure 6: first row: morphing with fast transition of details and slow transition of global features;
second row: morphing with slow transition of details and fast transition of global features

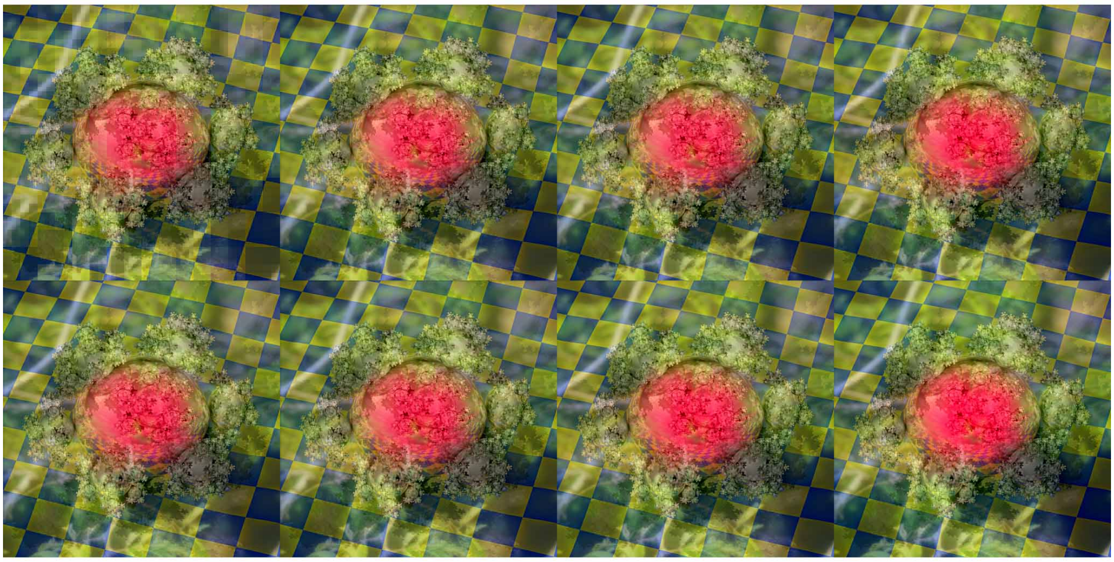

Figure 7: morphing with different wavelets: first row - Haar, biorthogonal spline wavelets (1,3) , (1,5), and (2,6);
second row - biorthogonal spline wavelet (3,3) , (3,7), Pseudocoiflets, and cubic Battle-Lemarié